RSC Advances

COMMUNICATION

View Article Online
View Journal | View Issue

Cite this: *RSC Adv.*, 2015, **5**, 88578

Received 20th August 2015
Accepted 12th October 2015

DOI: 10.1039/c5ra16817a

www.rsc.org/advances

Aggregation of low-concentration dirhamnolipid biosurfactant in electrolyte solution†

Hua Zhong,*[abc] Lei Yang,[ab] Xin Yang,[ab] Guangming Zeng,*[ab] Zhifeng Liu,[ab] Yang Liu[ab] and Xingzhong Yuan[ab]

Dynamic light scattering (DLS) and cryo-transmission electron microscopy (cryo-TEM) tests demonstrated aggregate formation for dirhamnolipid biosurfactant (diRL) at concentrations lower than surface-tension-based critical micelle concentration (CMC_{st}). An increase of diRL concentration and solution pH results in a decrease of the aggregate size at diRL concentrations below CMC_{st}, whereas it has no influence at diRL concentrations above CMC_{st}. The cryo-TEM micrographs show spherical morphology of the aggregates, and the logarithm of aggregate size follows Gaussian distribution. The aggregates are negatively charged. The zeta potential of the aggregates decreases with an increase of diRL concentration to CMC_{st}, and stabilizes at diRL concentrations higher than CMC_{st}. An increase of the solution pH causes a decrease of the zeta potential. A transitional state assumption is raised for the interpretation of the diRL aggregation behavior. The results demonstrate formation of aggregates at significantly low diRL concentrations, which is of importance for the cost-effective application of rhamnolipid biosurfactants.

1 Introduction

Biosurfactants are surfactants produced by microbes. Due to expanding applications of biosurfactants in many fields, *e.g.* biomedicine and bioremediation, their aggregation behaviour in electrolytes has received much attention in recent years.[1–3] The aggregates have a variety of microstructures, including spherical, globular or cylindrical micelles,[1,4–8] spherical or irregular vesicles,[2,9,10] tubular or irregular bilayers,[11] and lamellar sheets.[3,12,13] Also, the lyotropic liquid crystalline phases with lamellar, hexagonal and cubic aggregate morphologies are observed at high surfactant concentrations.[14] The morphology of these aggregates has been demonstrated to be affected by surfactant concentration,[8,15] pH,[4,10,16] temperature,[12] counter-ions,[1,10,15] and ionic strength.[17]

Rhamnolipid is the most widely studied biosurfactant and its aggregates exhibit versatile structures at concentrations higher than the critical micelle concentration (CMC). For example, Ishigami *et al.* investigated the effect of solution pH on rhamnolipid aggregate structure at concentrations of 500–20 000 mg L^{-1} in phosphate buffered saline solution. The result showed that the aggregates existing in form of bilayers vesicle at pH of 4.3–5.8, bilayer lamella with pH rising to 6.0–6.5, and micelles with further increase of pH to 6.8.[18] Champion *et al.* determined the rhamnoliopid aggregate morphology at various pH at the concentration of 60 mM by cryo-TEM. The results show that aggregate phase transitioned in an order of bilayer lamella, large vesicles, small vesicles and micelle with the increase of pH.[4] In addition, transformation of dirhamnolipid aggregations from large particles into small particles with the increase of concentration at fixed pH has also been reported.[19]

All these prior researches, however, were almost implemented with surfactant concentrations far higher than CMC. However, there are studies showing that rhamnolipid exhibited excellent HOC-solubilization activity at significantly low concentrations. For example, rhamnolipid can enhance the solubility of hexadecane and octadecane by 3–4 orders of magnitude at concentrations lower than CMC determined by surface tension method, and such solubilization efficiency is much higher than at concentrations above CMC.[16,20] Hypothetically these HOC-solubilization activities of rhamnolipid surfactant may be related to its aggregation behavior at low concentrations, *e.g.* lower than CMC. Furthermore, signs of aggregate formation at concentrations lower than CMC for

[a]*College of Environmental Science and Engineering, Hunan University, Changsha 410082, P. R. China. E-mail: zhonghua@email.arizona.edu; zgming@hnu.edu.cn; whwyanglei@126.com; yx2013@hnu.edu.cn; lzf18182002@163.com; liuyang_feiyang@163.com; yxz@hnu.edu.cn*

[b]*Key Laboratory of Environmental Biology and Pollution Control (Hunan University), Ministry of Education, Changsha 410082, P. R. China*

[c]*Department of Soil, Water and Environment Science, The University of Arizona, Tucson, AZ 85721, USA*

† Electronic supplementary information (ESI) available: Electrical conductivity *versus* diRL concentration profile, typical number PSD profiles generated by Malvern DTS Nano software, DLS diffusion coefficient *versus* diRL concentration profile, and the cryo-TEM images used for aggregate size distribution analysis. See DOI: 10.1039/c5ra16817a

multi-component rhamnoliplids were observed using dynamic lighter scattering method.[7,15] Formation of premicelles for a variety of surfactants also have been reported.[21–24] These observations indicate the probability of sub-CMC aggregate formation for rhamnolipid, which still remains unexplored.

In this study, the aggregation behavior of dirhamnolipid in phosphate buffered electrolyte solution with concentrations near surface-tension-based CMC (or CMC_{st}) was investigated. The objective of this study is to examine whether rhamnolipid forms aggregate at concentrations below CMC_{st}, and to explore the effect of solution conditions on aggregate formation at low rhamnolipid concentration range.

2 Materials and methods

2.1 Biosurfactant and chemicals

The dirhamnolipid biosurfactant was produced, extracted, purified, and characterized using the method described by Zhong *et al.*[25] NaOH and HCl (analytical chemistry grade) were purchased from Damao Chemical (Tianjin, China). All other chemicals ($NaNO_3$, KH_2PO_4, $Na_2HPO_4 \cdot 12H_2O$, $MgSO_4$, $FeSO_4 \cdot 7H_2O$) were analytical chemistry grade with purity >99% and purchased from Sinopharm (Beijing, China).

2.2 Determination of CMC_{st}

The stock solution of the diRL were prepared in phosphate buffered saline solution (PBSS, $NaNO_3$ 2 g L^{-1}, KH_2PO_4 1.5 g L^{-1}, $Na_2HPO_4 \cdot 12H_2O$ 1.5 g L^{-1}, $MgSO_4$ 0.1 g L^{-1}, $FeSO_4 \cdot 7H_2O$ 0.01 g L^{-1}). PBSS solutions of diRL in a series of concentrations were prepared using dilution method. Surface tension of diRL solutions was measured at 30 °C with surface tensiometer (JZ-200A, Chengde, China) using the Du Noüy Ring method. CMC_{st} of diRL was obtained from the relation of surface tension and diRL concentration using the scheme described by Yuan *et al.*[26] Electrical conductivity of diRL solutions was measured with DDS-11A Conductivity Meter (Shengci, Shanghai, China).

2.3 Hydrodynamic aggregate size and zeta potential

pH of PBSS solutions of diRL was adjusted to 8.0 with 20% NaOH solution using a capillary glass pipe. High concentration of NaOH was used to minimize change of solution volume during pH adjustment. These solutions were then filtered through a 0.22 μm filter (Millex-HV, Millipore, Billerica, Ma, US) to remove suspended solid particles that may interfere with the measurement. Results of preliminary test showed that the size of rhamnolipid aggregates is far less than 0.22 μm at pH 8.0, so they will not be retained by filtering. The solutions were allowed to stand still for 2 h. Then pH of the solutions was adjusted in sequence to 7.5, 7.0, 6.5, or 6.0 with 20% hydrochloric acid. For each sample, aggregate size and zeta potential were measured using Zetasizer Nano ZEN3600 (Malvern Instruments, U.K.).

The aggregate particle size was determined based on dynamic light scattering (DLS) mechanism using He–Ne laser at wavelength of 623 nm and working power of 4.0 mW. 1 ml of the sample was loaded to the DTS-0012 cell and measured at temperature of 30 °C. The scattered light was collected by receptor at angle of 173° from light path. A mean size provided by DTS Nano software (Malvern Instruments, U.K.) was used to represent the aggregate size of the sample. Also, the number-based particle size distribution (number PSD) data generated by the software were used for the statistical analysis of aggregate size. The diffusion coefficient of the aggregates was generated by the software.

The zeta potential measurement is based on the mechanism of particle electrophoresis in aqueous solution. 1 mL sample is loaded to DTS 1060 folded capillary cell and the electrophoretic mobility of the aggregate was measured at 30 °C under automatic voltage using a laser Doppler velocimetry with M3-PALS technique to avoid electroosmosis. The measured data was converted into corresponding zeta potential by applying the Helmholtz–Smoluchowski equation.[27]

2.4 Cryo-transmission electron microscopy test

diRL solution or electrolyte solution in the absence of diRL in volume of 4 μL was placed on the grid with a holy polymer film using a microsyringe, and then sent to a FEI Vitrobot sample plunger system (FEI, Hillsboro, Oregon). Excessive sample was removed by a filter paper. Then the sample grid was rapidly vitrified in liquid ethane and transferred to a liquid nitrogen bath. The morphology of diRL aggregate were then viewed and photographed on a Tecnai F20 transmission electron microscope (FEI, Hillsboro, Oregon) at an acceleration voltage of 120 kV. Nano measurer 1.2.5 software (Shanghai, Fudan University) was used to process the micrograph images. The program marked the recognized particles in an image with circles. The diameter of every circle was measured by pairing the circle to a screen ruler calibrated by the reference bar in the image and used as the size of the particle. In order to obtain statistically representative sample for aggregate size distribution analysis, the size data were collected on more than 100 or 200 particles from multiple images for rhamnolipid concentrations of 25 or 250 μM, respectively.

3 Results and discussion

For all the pHs, surface tension of the solution decrease significantly with the increase of rhamnolipid concentration at low surfactant concentrations, and then further increase of surfactant concentration has no significant effect on surface tension (Fig. 1). Based on the method of Yuan *et al.*,[26] the CMC_{st} values obtained are 62, 78, 82, 83 and 82 μM for pH of 6.0, 6.5, 7.0, 7.5 and 8.0, respectively. The result showed that the increase of solution pH resulted in increase of diRL CMC_{st} for pH not higher than 7.0. The electrical conductivity of diRL solution increased with the increase of diRL concentration for all pH conditions, however, the two-line profile with a distinguishable slope inflection is not observed for any of the curves (Fig. S1a, ESI†). The plot of conductivity derivative *versus* diRL concentration is presented in Fig. S1b, ESI.† The conductivity derivative shows a gradual decrease at the concentration below CMC_{st}, which is in contrast to an abrupt decrease at CMC generally for regular surfactants.

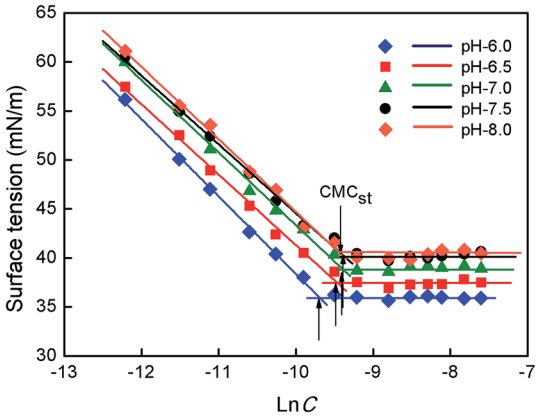

Fig. 1 Surface tension *versus* diRL concentration in PBSS solution and determination of CMC_{st}.

Results of DLS-size measurement show that diRL aggregates were detected at diRL concentration both below and above CMC_{st}. The number PSD profiles generated by Malvern DTS Nano software show only one peak for all the conditions of measurements (typical profiles are presented in Fig. S2, ESI†), indicating presence of only one type of aggregate. The influence of diRL concentration and solution pH on aggregate size is shown in Fig. 2a. The aggregate size is in a range of 8 to 72 nm. When the solution pH is not higher than 7.0, the aggregate size decreased with the increase of diRL concentration up to 100 μM. At diRL concentrations ranging from 10 to 100 μM (close to CMC_{st}), the aggregate size decreases rapidly with increase of pH. When diRL concentration is higher than 100 μM, both diRL concentration and pH have no observable influence on the aggregate size. The relation between DLS diffusion coefficients and diRL concentrations is shown in Fig. S3, ESI.† The diffusion coefficient increases with increase of diRL concentration when the concentration is lower than CMC_{st}. This result is in contrast to DLS diffusion coefficient for regular surfactants, for which an abrupt decrease of the coefficient is observed at CMC.[28] This result, however, matches with the result of size measurement in that diffusion coefficient is larger for smaller particles.

Aggregate zeta potential variation with diRL concentration and pH is presented in Fig. 2b. Because rhamnolipid is an anionic surfactant with carboxyl group in the hydrophilic moiety of the molecule, dissociation of the carboxyl groups yields negatively-charged aggregate surface and hence negative zeta potential of the aggregates. For all the pHs, the zeta potential decreases significantly the increase of diRL concentration from 25 μM to 100 μM. Further increase of concentration has minimal influence. For all the diRL concentrations tested, increase in solution pH causes decrease in aggregate zeta potential. Increase of solution pH results in enhanced dissociation of diRL carboxyl group, which in turn increases the aggregate surface charge density and lowers zeta potential (provided a dissociation equilibrium constant of $10^{-5.6}$ for rhamnolipid carboxyl group at room temperature,[18] the dissociation rate of the rhamnolipid is 71.5, 88.8, 96.2, 98.8, 99.6% at pH of 6.0, 6.5, 7.0, 7.5, 8.0, respectively).

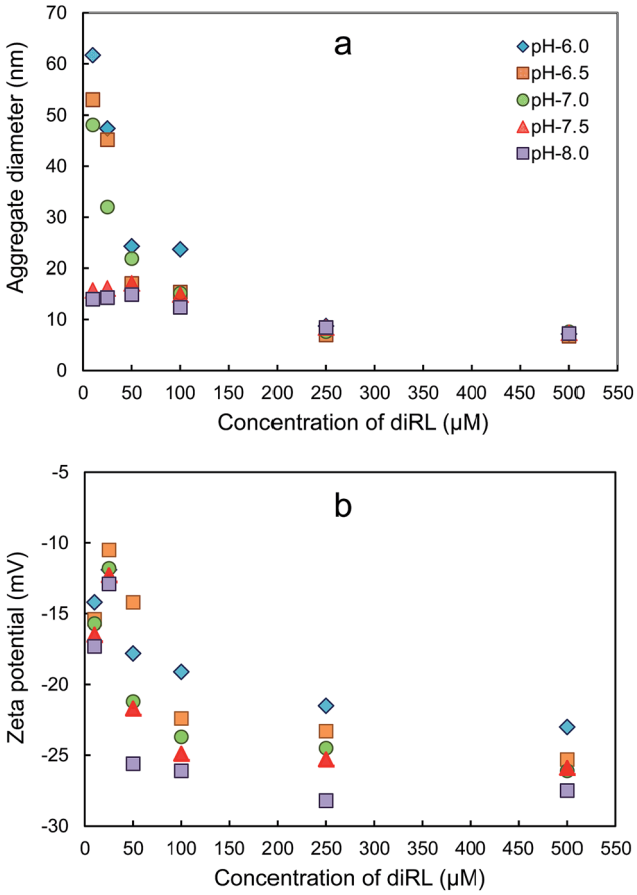

Fig. 2 DLS size (a) and zeta potential (b) of aggregates as a function of diRL concentration and solution pH.

25 μM (below CMC_{st}) and 250 μM (above CMC_{st}) of diRL solution at pH of 6.0 or 8.0 were examined using cryo-TEM. Typical images of the aggregates are presented in Fig. 3. Aggregates are observed for all the four conditions, which is in contrast to the observation in the absence of diRL for which no aggregates are observed (Fig. S4a, ESI†). The morphology of the aggregates is spherical with minimal transparency, indicating micelle-type structure. Other aggregate structures reported in literatures at relatively high rhamnolipid concentrations, *e.g.* vesicles, lamella or microtubes,[4,8,9,19] are not observed for any of the conditions tested. This is consistent with the result of DLS size measurement that only one type of aggregate is observed. The cryo-TEM result further confirms formation of diRL aggregates at concentrations below CMC. On the other hand, the DLS size and cryo-TEM results also shows that the aggregates are not premicelles, which are defined as dimers and low-aggregation number aggregates of surfactant molecules before micelle formation.[21–24]

All the cryo-TEM images used for aggregate size distribution analysis are shown in Fig. S4, ESI.† Gaussian distribution is commonly used to depict natural phenomena associated with real-valued random variables whose distributions are unknown. The distributions of aggregate sizes obtained with either DLS or cryo-TEM method appear to deviate from Gaussian distribution

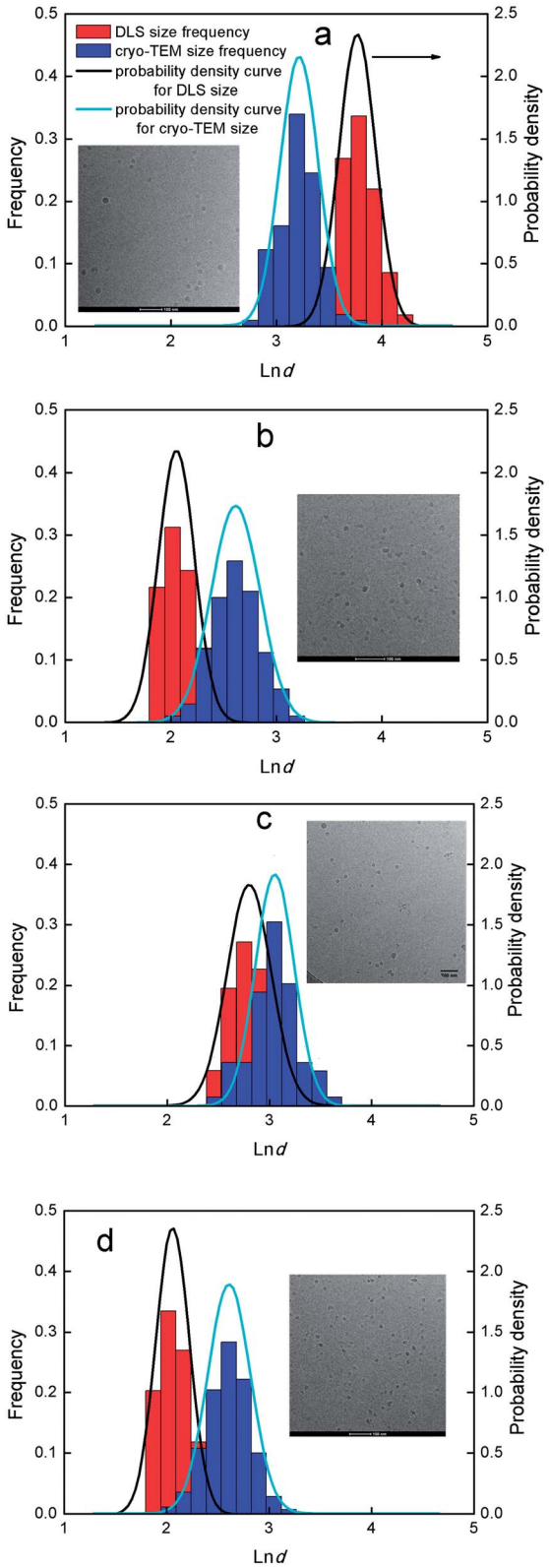

Fig. 3 Distribution of diRL aggregate size obtained using DLS and cryo-TEM methods and representative cryo-TEM micrographs of diRL aggregates formed in PBSS solution. (a) 25 μM, pH 6.0; (b) 250 μM, pH 6.0; (c) 25 μM, pH 8.0; (d) 250 μM, pH 8.0.

(data not shown), however, natural logarithm of the sizes follows Gaussian distribution very well for all the four conditions examined (Fig. 3). Values of the parameters for the fit are presented in Table 1. The mean of cryo-TEM size at diRL concentration of 25 μM (lower than CMC_{st}) is larger than at diRL concentration of 250 μM (higher than CMC_{st}), for pH of either 6.0 or 8.0. The cryo-TEM size at diRL concentration of 25 μM is larger for pH 6.0 than for pH 8.0, and they are identical at diRL concentration of 250 μM. These results show that change of the cryo-TEM size is similar to that of DLS size in terms of trend, indicating good consistency. The cryo-TEM sizes obtained at the condition of 25 μM diRL and pH 6.0 (24.9 nm) is significantly smaller than the DLS-based size (43.2 nm). The particle size obtained by DLS method is hydrodynamic diameter, which is the diameter of a sphere that has the same translational diffusion coefficient as the particle. This hydrodynamic size is usually larger than the real particle size.[29] Either the DLS size or the cryo-TEM size obtained at high diRL concentration (0.5 mM) in our study is smaller than that measured at similar concentrations using similar methods in the study of Guo and Hu,[8] in which formation of large vesicles was observed. The ionic strength of diRL solution in that study is approximately 10 mM, which is significantly lower than that in our study (55 mM with divalent ions). The hydrophilic head of diRL molecule contains a carboxylic group. At pH higher than 6.0, the majority of carboxylic groups are dissociated and negatively charged. Cations in the diRL electrolyte solution can easily bind with the carboxylate groups, resulting in the induction of the solvated groups and disfavours formation of large aggregates.[9] Such a conversion of large vesicles to small ones was also observed when Cd^{2+} was introduced in solution of rhamnolipid solution.[4] In addition, the dirhamnolipid used in the study of Guo and Hu contains higher ratio of long-chain species ($Rha_2C_{10}C_{12:1}$ and $Rha_2C_{10}C_{14:1}$. $Rha_2C_xC_{y(:z)}$ designates the diRL homologue with x and y as the carbon atom number of each aliphatic acid chain in the lipid moiety, and z as the number of unsaturated bonds in lipid moiety),[8] which results in stronger hydrophobic interaction between molecules and thus favours formation of large vesicles.

The diRL used in this study is not a pure compound comprising one species of molecule. Instead, it is a rhamnolipid mixture consisting of three homologues which are the same in

Table 1 Gaussian regression parameters for DLS and cryo-TEM aggregate size distribution

	DLS				cryo-TEM			
diRL sample	μ^a	σ^{2b}	R^2	d^c (nm)	μ	σ^2	R^2	d (nm)
25 μM, pH 6.0	3.77	0.031	1.00	**43.2**	3.22	0.033	0.96	**24.9**
250 μM, pH 6.0	2.05	0.030	0.97	**7.8**	2.61	0.053	0.98	**13.7**
25 μM, pH 8.0	2.80	0.046	0.98	**16.5**	3.05	0.033	0.97	**21.2**
250 μM, pH 8.0	2.06	0.027	0.98	**7.8**	2.61	0.044	1.00	**13.6**

[a] Mean of ln d obtained from Gaussian regression. [b] Variance of ln d obtained from Gaussian regression. [c] The mean aggregate size obtained using $d = e^{\mu}$.

structure of polar moiety (double rhamnose rings and a carboxylic group) while different in length of aliphatic chains ($Rha_2C_{10}C_{10}$, $Rha_2C_{10}C_{12:1}$ and $Rha_2C_{10}C_{12}$ with molar fractions of 0.70, 0.11 and 0.19, respectively).[25] We speculate that this multi-component nature of the diRL results in formation of aggregates at concentrations below CMC_{st}. The strength of hydrophobic interactions between diRL molecules with aliphatic chains of different lengths are not uniform, which may result in a transitional state for aggregation-related behavior, *e.g.* formation of aggregates in electrolyte solution before the solution surface is saturated with diRL (corresponding to diRL concentration of CMC_{st}), and graduality in change of electrical conductivity increasing rate. In the transitional state, increase in diRL solution concentration may enhance partition of diRL molecules to aggregates and therefore increase the density of the molecules in aggregate. Increase of solution pH results in enhanced dissociation of diRL molecules. Both effects enhance the electrostatic repulsion between polar moieties of diRL molecules in aggregates and hence the curvature of aggregates. As a result, when diRL concentrations are lower than CMC_{st} (the transitional state) the aggregate size decreases with increase of the concentration and solution pH.

4 Conclusions

DLS and cryo-TEM methods were used to study aggregation behavior of low-concentration diRL and the results demonstrated formation of aggregates at concentrations below CMC_{st}. The effect of diRL concentration and solution pH on aggregate size and zeta potential is significant when diRL concentration is lower than the CMC_{st}. The multicomponent nature of the diRL and consequently a transitional state are supposed to be responsible for these aggregation behaviors at low diRL concentrations. Also, results of the study indicate that the surface-tension-based CMC may not be used as the concentration defining aggregate formation for multicomponent biosurfactants. This work is of importance for cost-effective application of rhamnolipid. Further researches should be focused on validating the transitional state speculation and characterizing the rhamnolipid aggregates in transitional state in more detail.

Acknowledgements

The authors thank National Laboratory for physical sciences, University of Science and Technology of China, for implementing cryo-TEM tests. This study was funded by the National Natural Science Foundation of China (51378192, 51378190, 51308200 and 21276269).

References

1 K. Matsuoka, K. Takagi and C. Honda, *Chem. Phys. Lipids*, 2013, **172**, 6–13.
2 J. Arutchelvi, J. Sangeetha, J. Philip and M. Doble, *Colloids Surf., B*, 2014, **116**, 396–402.
3 X. Dai, H. Ding, Q. Yin, G. Wan, X. Shi and Y. Qiao, *J. Mol. Graphics Modell.*, 2015, **57**, 20–26.
4 J. T. Champion, J. C. Gilkey, H. Lamparski, J. Retterer and R. M. Miller, *J. Colloid Interface Sci.*, 1995, **170**, 569–574.
5 D. Song, Y. Li, S. Liang and J. Wang, *Colloids Surf., A*, 2013, **436**, 201–206.
6 M. Chen, C. Dong, J. Penfold, R. K. Thomas, T. J. Smyth, A. Perfumo, R. Marchant, I. M. Banat, P. Stevenson, A. Parry, I. Tucker and I. Grillo, *Langmuir*, 2013, **29**, 3912–3923.
7 H. Abbasi, K. A. Noghabi, M. M. Hamedi, H. S. Zahiri, A. A. Moosavi-Movahedi, M. Amanlou, J. A. Teruel and A. Ortiz, *Colloids Surf., B*, 2013, **101**, 256–265.
8 Y. P. Guo and Y. Y. Hu, *Colloids Surf., A*, 2014, **445**, 12–20.
9 O. Pornsunthorntawee, S. Chavadej and R. Rujiravanit, *Colloids Surf., B*, 2009, **72**, 6–15.
10 Z. A. Raza, Z. M. Khalid, M. S. Khan, I. M. Banat, A. Rehman, A. Naeem and M. T. Saddique, *Biotechnol. Lett.*, 2010, **32**, 811–816.
11 E. Haba, A. Pinazo, R. Pons, L. Perez and A. Manresa, *Biochim. Biophys. Acta, Biomembr.*, 2014, **1838**, 776–783.
12 Ş. Ş. Helvacı, S. Peker and G. Özdemir, *Colloids Surf., B*, 2004, **35**, 225–233.
13 W. Worakitkanchanakul, T. Imura, T. Fukuoka, T. Morita, H. Sakai, M. Abe, R. Rujiravanit, S. Chavadej, H. Minamikawa and D. Kitamoto, *Colloids Surf., B*, 2008, **65**, 106–112.
14 P. K. Vinson, Y. Talmon and A. Walter, *Biophys. J.*, 1989, **56**, 669.
15 Y. P. Guo, Y. Y. Hu, R. R. Gu and H. Lin, *J. Colloid Interface Sci.*, 2009, **331**, 356–363.
16 Y. M. Zhang and R. M. Miller, *Appl. Environ. Microbiol.*, 1992, **58**, 3276–3282.
17 M. Hofer, R. Y. Hampton, C. R. Raetz and H. Yu, *Chem. Phys. Lipids*, 1991, **59**, 167–181.
18 Y. Ishigami, Y. Gama, H. Nagahora, M. Yamaguchi, H. Nakahara and T. Kamata, *Chem. Lett.*, 1987, **16**, 763–766.
19 M. Sánchez, F. J. Aranda, M. J. Espuny, A. Marqués, J. A. Teruel, Á. Manresa and A. Ortiz, *J. Colloid Interface Sci.*, 2007, **307**, 246–253.
20 H. Zhong, Y. Liu, Z. F. Liu, Y. B. Jiang, F. Tan, G. M. Zeng, X. Z. Yuan, M. Yan and Q. Y. Niu, *Int. Biodeterior. Biodegrad.*, 2014, **94**, 152–159.
21 L. D. Song and M. J. Rosen, *Langmuir*, 1996, **12**, 1149–1153.
22 K. Tsubone, Y. Arakawa and M. J. Rosen, *J. Colloid Interface Sci.*, 2003, **262**, 516–524.
23 Q. Miao, Y. Jin, Y. Dong, Z. F. Cao and B. Zhang, *J. Polym. Res.*, 2010, **17**, 911–921.
24 D. N. LeBard, B. G. Levine, R. deVane, W. Shinoda and M. L. Klein, *Chem. Phys. Lett.*, 2012, **522**, 38–42.
25 H. Zhong, G. M. Zeng, J. X. Liu, X. M. Xu, X. Z. Yuan, H. Y. Fu, G. H. Huang, Z. F. Liu and Y. Ding, *Appl. Microbiol. Biotechnol.*, 2008, **79**, 671–677.
26 X. Z. Yuan, F. Y. Ren, G. M. Zeng, H. Zhong, H. Y. Fu, J. Liu and X. M. Xu, *Appl. Microbiol. Biotechnol.*, 2007, **76**, 1189–1198.
27 R. J. Zasoski, in *Encyclopedia of Soil Science*, ed. W. Chesworth, Springer, Netherlands, 2008, pp. 841–845.
28 B. Das, B. maitra, S. M. Mercer, M. Everist and D. G. Leaist, *Phys. Chem. Chem. Phys.*, 2008, **10**, 3083–3092.
29 S. Pabisch, B. Feichtenschlager, G. Kickelbick and H. Peterlik, *Chem. Phys. Lett.*, 2012, **521**, 91–97.

